Eur. Phys. J. C (2023) 83:136
https://doi.org/10.1140/epjc/s10052-023-11282-8

THE EUROPEAN PHYSICAL JOURNAL C

Regular Article - Theoretical Physics

Semileptonic *b*-baryon decays within a new physics approach

C. P. Haritha, Karthik Jain, Barilang Mawlong[a]

School of Physics, University of Hyderabad, Hyderabad 500046, India

Received: 5 August 2022 / Accepted: 30 January 2023 / Published online: 10 February 2023

Abstract The excess in the measurement of the branching fractions of $\bar{B} \to D(D^*)\tau^-\bar{\nu}_\tau$ and $B_c \to J/\psi\tau^-\bar{\nu}_\tau$ from the standard model expectation hints the existence of new physics beyond the standard model. Motivated by these indications, we study similar modes mediated by $b \to c\tau\bar{\nu}_\tau$ transitions, in particular, the semileptonic b-baryon decay modes $\Xi_b \to \Xi_c\tau^-\bar{\nu}_\tau$ and $\Sigma_b \to \Sigma_c^{(*)}\tau^-\bar{\nu}_\tau$. We consider a general low energy effective Hamiltonian approach, which includes both standard model and new physics contributions. Within different new physics scenarios, we investigate the impact of the new contributions on these modes and present predictions for various semileptonic q^2-spectra.

1 Introduction

The standard model (SM) of particle physics provides a unified framework of the fundamental particles and their interactions. Although the SM has been successful in describing a wide range of experimental measurements, it is not a complete theory. The limitations of the SM have led to various new physics (NP) beyond the SM searches via both direct and indirect means. NP has been hinted by precision measurements such as that of the muon anomalous magnetic moment $(g-2)_\mu$. Flavor anomalies observed in b-hadron decays represent one of the indirect indications of NP beyond the SM. A number of measurements of b-decay observables have been found to disagree with SM predictions. These discrepancies have been seen particularly in decays mediated by $b \to s\ell^+\ell^-$ and $b \to c\tau^-\bar{\nu}_\tau$ transitions.

One of the key properties of the SM is lepton flavor universality (LFU) which states that the couplings of leptons to gauge bosons are flavor independent. In the b sector, some of the observables that have been found to violate LFU are the ratio of branching fractions R_D and $R_{D^{(*)}}$ which are defined as, $R_{D^{(*)}} = \mathcal{B}(B \to D^{(*)}\tau\nu)/\mathcal{B}(B \to D^{(*)}\ell\nu)$, with $\ell = e$ or μ. The world average values $R_D^{expt} = 0.339 \pm 0.026 \pm 0.014$ and $R_{D^*}^{expt} = 0.295 \pm 0.010 \pm 0.010$ [1] exceed their SM predictions $R_D^{\rm SM} = 0.299 \pm 0.003$ and $R_{D^*}^{SM} = 0.254 \pm 0.005$ [2–7] by 1.4σ and 2.8σ, respectively. The ratio of branching fractions $R_{J/\psi} = \mathcal{B}(B_c \to J/\psi\tau\nu_\tau)/\mathcal{B}(B_c \to J/\psi\mu\nu_\mu) = 0.71 \pm 0.17 \pm 0.18$ as measured by the LHCb collaboration [8] also deviates from the SM prediction $R_{J/\psi}^{\rm SM} = 0.289 \pm 0.01$ [9] by about 2σ. These observations suggest the presence of NP beyond the Standard Model (SM) and motivate the study of other decays mediated by the same $b \to c\tau^-\bar{\nu}_\tau$ transitions. The τ polarization $P_\tau^{D^*} = -0.38 \pm 0.51\ ^{+0.21}_{-0.16}$ [10,11] and the D^{*-} polarization $F_L^{D^*} = 0.60 \pm 0.08 \pm 0.04$ [12] as measured by the Belle collaboration also provide additional aspects to analyse NP in these transitions.

To explain the anomalies in the B meson modes, various NP models have been proposed, some of which can be found in [13–21]. In our work, we analyse the semileptonic $b \to c\tau^-\bar{\nu}_\tau$ transitions involving heavy b-baryons, $B_b \to B_c\tau^-\bar{\nu}_\tau$, where $B_b = \Xi_b, \Sigma_b$ and $B_c = \Xi_c, \Sigma_c^{(*)}$, in a model-independent approach. The semileptonic decays of b-baryons have not been studied as extensively as the b-meson ones though. Insights on weak interaction properties of the heavy baryons, the underlying dynamics and sensitivity to NP can be obtained from such decays. The semileptonic heavy b-baryon decays can also complement the sensitivity search of NP to that of the meson modes. The b-baryon decay modes which are of half-integer spin provide an auxiliary environment to test the observed anomalies. In addition, the CKM matrix parameter V_{cb} can be determined from the semileptonic decays of heavy baryons mediated by $b \to c\tau^-\bar{\nu}_\tau$ transitions complimentary to heavy meson semileptonic decays. Decays involving heavy baryons are also good grounds for obtaining information on heavy quark physics. There is also less contamination from non-

[a] e-mail: barilang05@gmail.com (corresponding author)

perturbative QCD effects with regards to semileptonic decays as leptons are involved. From the experimental side, experiments such as the Tevatron and LHC have made significant progress in the study of heavy baryons containing a b quark with a considerable accumulation of data. For the baryons of interest in this work, the Ξ_b^0 and $\Xi_b^\pm$ baryons were first observed by CDF and D0 [22,23]. LHCb [24–32] and CDF [33] have also measured their masses, lifetimes and branching ratios. Clear signals of four strongly-decaying baryon states, Σ_b^+, $\Sigma_b^{*+}(uub)$, Σ_b^-, $\Sigma_b^{*-}(ddb)$, have been obtained by CDF [34,35] and LHCb [36]. Since the Σ_b baryon predominantly decays via the strong interaction, it may be difficult to measure its weak branching fraction. However, analysing the semileptonic decay modes may be insightful as they can be more sensitive to new particles and any deviation from the SM prediction will be a clear indication of NP [37].

The experimental progress in the study of heavy b-baryons which contain a single heavy quark necessitates theoretical progress. Important theoretical studies on b-baryons and their decays have indeed been carried out [38–40]. The semileptonic mode involving the spin-1/2 baryon Λ_b has been considerably studied. The form factors of $\Lambda_b \to \Lambda_c$ mode have been computed using lattice QCD (LQCD) [41]. Exclusive semileptonic decays of spin-1/2 baryons $\Lambda_b, \Omega_b, \Sigma_b, \Xi_b$ have been examined in the spectator quark model [42], the relativistic three-quark model [39] and a non-relativistic quark model [43]. The decay modes $\Lambda_b \to \Lambda_c \ell^- \bar{\nu}_\ell$ and $\Xi_b \to \Xi_c \ell^- \bar{\nu}_\ell$ were analysed in [44] within a light-front constituent quark model and similarly in [45] within a combined non-relativistic constituent quark model and heavy quark effective theory study. The authors in [46] studied the weak transition of $\Sigma_b \to \Sigma_c$ and $\Omega_b \to \Omega_c$ in the light-front quark model considering the quark–diquark picture for heavy baryons. Similarly, in [37], the authors studied the $\Lambda_b \to \Lambda_c$ and $\Sigma_b \to \Sigma_c$ weak decays in the light-front quark model by considering the two spectator light quarks as individual ones rather than a diquark. In the work of [47], the semileptonic decays of heavy baryons (Λ_b, Σ_b, Ω_b, Ξ_b, $\Xi_b^{'}$) with scalar and axial-vector diquarks in the relativistic quark model framework were analysed. The semileptonic decays $\Xi_b \to \Xi_c \ell^- \nu_\ell$ and $\Xi_b \to \Lambda \ell^- \nu_\ell$ were analysed in the framework of the relativistic quark–diquark model based on the quasipotential approach in [48]. In these works, SM estimates of decay rates, branching fractions, longitudinal and transverse asymmetries, the longitudinal to transverse decay ratio, the CKM parameter $|V_{cb}|$ and various other asymmetry parameters such as forward-backward asymmetry, convexity parameter, polarizations of the daughter baryon and the charged lepton, and ratio of branching fractions were determined.

There have also been some model-independent studies to probe NP in the heavy baryon decays. The $\Lambda_b \to \Lambda_c \tau^- \bar{\nu}_\tau$ mode has already been analysed with several NP signatures such as those that can be found in [49–63]. In [64], the mode $\Xi_b \to \Xi_c \tau^- \bar{\nu}_\tau$ decay was analyzed in the SM and in various NP scenarios with vector and scalar type of interactions. The observables R_D and R_{D^*} were used to constrain the NP parameter space. The decay modes $\Sigma_b \to \Sigma_c \ell^- \bar{\nu}_\ell$ and $\Omega_b \to \Omega_c \ell^- \bar{\nu}_\ell$ were analyzed similarly in [65] within a model-independent effective field theory formalism. Real vector and scalar NP couplings were considered and the allowed NP parameter space was obtained from the experimental values of the observables $R_{D^{(*)}}$. In [66], new physics was probed in the baryon decays $\Xi_b \to \Lambda(\Xi_c)\tau^- \bar{\nu}_\tau$. The new couplings assumed to be complex were constrained using the experimental measurements of $\mathcal{B}(B_c^+ \to \tau^+ \nu_\tau)$, R_π^l, R_{D^*}, $R_{J/\psi}$ and $F_L^{D^*}$. The authors in [67] studied the decay modes $\Sigma_b \to \Sigma_c \ell^- \bar{\nu}_\ell$ and $\Omega_b \to \Omega_c \ell^- \bar{\nu}_\ell$ in a model-independent effective field theory formalism. The NP couplings were assumed to be complex and the allowed NP parameter space was constrained from the experimental values of the observables $\mathcal{B}(B \to D^{(*)} \ell^- \bar{\nu}_\ell)$, $R_{D^{(*)}}$, $R_{J/\psi}$. In these analyses, predictions for various q^2-dependent observables such as differential decay rate, branching fraction, forward-backward asymmetry of the charged lepton, convexity parameter, ratio of branching fractions, polarizations of the daughter baryon and the charged lepton were presented.

In our analysis of the heavy b-baryon semileptonic decay modes $\Xi_b \to \Xi_c \tau^- \bar{\nu}_\tau$ and $\Sigma_b \to \Sigma_c^{(*)} \tau^- \bar{\nu}_\tau$, we consider a model-independent effective field theory framework, with a low energy effective Hamiltonian that includes both SM and NP contributions. For the amplitudes of the semileptonic decays of heavy b-hadrons, the hadronic matrix elements of weak currents are generally parametrized in terms of form factors that embody nonperturbative QCD effects. For $b \to c$ transitions, the heavy quark effective theory (HQET) [68–75] which is based on the $1/m_Q$ expansion of the QCD Lagrangian and heavy quark symmetry, is the right approach for hadrons containing a single heavy quark. In HQET, the form factors can be simplified and described by the universal Isgur–Wise functions in the heavy quark expansion. Here, we analyze the decay modes without taking into account effects of radiative corrections to the HQET form factors. In our work, we use these form factors which have been obtained in the relativistic quark model (RQM) framework of [47], with the quark–diquark picture where a heavy baryon is seen as a bound state of a heavy quark and a light diquark system. We also use helicity amplitude formalism [76–78] to analyze the semileptonic transitions $\Xi_b \to \Xi_c \tau^- \bar{\nu}_\tau$ and $\Sigma_b \to \Sigma_c^{(*)} \tau^- \bar{\nu}_\tau$. For the new couplings, we obtain constraints using the experimental measurements of $R_{D^{(*)}}$, $R_{J/\psi}$, $F_L^{D^*}$, $P_\tau^{D^*}$ and the upper bound of $\mathcal{B}(B_c^+ \to \tau^+ \nu_\tau)$. We then investigate the impact of these new contributions and present the predictions for various q^2-

dependent observables. It is to be noted that new physics sensitivity of the $\Sigma_b \to \Sigma_c^* \tau^- \bar{\nu}_\tau$ mode has not been investigated so far. The helicity amplitudes in the presence of NP for this $1/2^+ \to 3/2^+$ transition has been worked out thoroughly and presented here.

The paper is organized as follows. In Sect. 2, we briefly discuss the theoretical framework used for the analysis, including form factors and helicity amplitudes. We also define various q^2-dependent observables in this section. To assess the validity of the RQM framework, we first compare the theoretical predictions obtained using RQM with those obtained using lattice QCD results in Sect. 3. In Sect. 4, we present and discuss the NP sensitivity of the q^2-dependent observables for the $\Xi_b \to \Xi_c \tau^- \bar{\nu}_\tau$ and $\Sigma_b \to \Sigma_c^{(*)} \tau^- \bar{\nu}_\tau$ decay modes, considering one new coupling at a time and also using the global fits of [54]. We summarize our findings and conclude in Sect. 5.

2 Theoretical framework

We consider the most general low energy effective Hamiltonian relevant for $b \to c\ell^- \bar{\nu}_\ell$ transitions at the b-quark mass scale, with only left-handed neutrinos, given by [54]

$$\mathcal{H}_{eff} = \frac{4G_F}{\sqrt{2}} V_{cb} \Big[\left(1 + C_{V_L}\right) \mathcal{O}_{V_L} + C_{V_R} \mathcal{O}_{V_R} + C_{S_R} \mathcal{O}_{S_R} + C_{S_L} \mathcal{O}_{S_L} + C_T \mathcal{O}_T \Big] + \text{h.c.}, \tag{1}$$

where G_F is the Fermi constant and V_{cb} is the CKM matrix element. The fermionic operators are given by

$$\begin{aligned} \mathcal{O}_{V_{L,R}} &= \left(\bar{c}\gamma^\mu b_{L,R}\right)\left(\bar{\ell}_L \gamma_\mu \nu_{\ell_L}\right) \\ \mathcal{O}_{S_{L,R}} &= \left(\bar{c} b_{L,R}\right)\left(\bar{\ell}_R \nu_{\ell_L}\right) \\ \mathcal{O}_T &= \left(\bar{c}\sigma^{\mu\nu} b_L\right)\left(\bar{\ell}_R \sigma_{\mu\nu} \nu_{\ell_L}\right) \end{aligned} \tag{2}$$

and their corresponding Wilson coefficients denoted by $C_{V_{L,R}}, C_{S_{L,R}}, C_T$ are the vector, scalar and tensor type couplings that encode the NP contributions. The new contributions are assumed to be present only in the $\ell = \tau$ mode as indicated by the LFU ratios. In our analysis, we consider only vector and scalar type of interactions and the NP couplings are assumed to be real. It has been shown that within the context of the SM effective field theory (SMEFT) [79–81], the vector operator with a right-handed quark current does not contribute to LFU violation [54,55,82–84]. Hence, we do not include the effects of C_{V_R} in our work.

2.1 Hadronic matrix elements and form factors

The hadronic matrix elements of the vector and axial vector currents for the decays $B_b \to B_c^{(*)} \ell^- \bar{\nu}_\ell$ can be parametrized in terms of various form factors expressed as functions of velocities of baryons [47].

For $1/2 \to 1/2$ transition, the parametrization is given by

$$\begin{aligned} M_V^\mu &= \langle B_c(v', s')|\bar{c}\gamma^\mu b|B_b(v, s)\rangle \\ &= \bar{u}_{B_c}(v', s')\Big[F_1(\omega)\gamma^\mu + F_2(\omega)v^\mu + F_3(\omega)v'^\mu\Big] \\ &\quad \times u_{B_b}(v, s), \\ M_A^\mu &= \langle B_c(v', s')|\bar{c}\gamma^\mu\gamma_5 b|B_b(v, s)\rangle \\ &= \bar{u}_{B_c}(v', s')\Big[G_1(\omega)\gamma^\mu + G_2(\omega)v^\mu + G_3(\omega)v'^\mu\Big] \\ &\quad \times \gamma_5 u_{B_b}(v, s), \end{aligned} \tag{3}$$

where B_b represent the bottomed baryons Ξ_b, Σ_b and B_c represent the charmed baryons Ξ_c, $\Sigma_c^{(*)}$, and u_{B_b} and $\bar{u}_{B_c}$ are the Dirac spinors of B_b and B_c, respectively. The form factors $F_1, F_2, F_3, G_1, G_2, G_3$ are functions of the velocity transfer variable $\omega = v \cdot v' = \frac{(m_{B_b}^2 + m_{B_c}^2 - q^2)}{2m_{B_b} m_{B_c}}$, where v and v' are the four-velocities of the baryons B_b and B_c, respectively.

Using equations of motion, the hadronic matrix elements of the scalar and pseudoscalar currents can be obtained from those of the vector and axial vector currents and are given by

$$\begin{aligned} \langle B_c(v', s')|\bar{c}b|B_b(v, s)\rangle &= \frac{q_\mu}{m_b - m_c} \\ &\quad \times \langle B_c(v', s')|\bar{c}\gamma^\mu b|B_b(v, s)\rangle \\ &= \bar{u}_{B_c}(v', s')\Bigg[F_1(\omega)\frac{\not{q}}{(m_b - m_c)} \\ &\quad + F_2(\omega)\left(\frac{m_{B_b}^2 - m_{B_c}^2 + q^2}{2m_{B_b}(m_b - m_c)}\right) \\ &\quad + F_3(\omega)\left(\frac{m_{B_b}^2 - m_{B_c}^2 - q^2}{2m_{B_c}(m_b - m_c)}\right)\Bigg] \\ &\quad \times u_{B_b}(v, s), \\ \langle B_c(v', s')|\bar{c}\gamma_5 b|B_b(v, s)\rangle &= \frac{q_\mu}{-(m_b + m_c)} \\ &\quad \times \langle B_c(v', s')|\bar{c}\gamma^\mu\gamma_5 b|B_b(v, s)\rangle \\ &= \bar{u}_{B_c}(v', s')\Bigg[-G_1(\omega)\frac{\not{q}}{(m_b + m_c)} \\ &\quad - G_2(\omega)\left(\frac{m_{B_b}^2 - m_{B_c}^2 + q^2}{2m_{B_b}(m_b + m_c)}\right) \\ &\quad - G_3(\omega)\left(\frac{m_{B_b}^2 - m_{B_c}^2 - q^2}{2m_{B_c}(m_b + m_c)}\right)\Bigg] \\ &\quad \times \gamma_5 u_{B_b}(v, s), \end{aligned} \tag{4}$$

where m_b and m_c denote the mass of b and c quarks respectively evaluated at the renormalization scale, $\mu = m_b$.

For $1/2 \to 3/2$ transition, the parametrization is given by

$$\begin{aligned} M_V^\mu &= \langle B_c^*(v', s')|\bar{c}\gamma^\mu b|B_b(v, s)\rangle \\ &= \bar{u}_{B_c^*,\lambda}(v', s')\Big[N_1(\omega)v^\lambda\gamma^\mu + N_2(\omega)v^\lambda v^\mu \end{aligned}$$

$$+N_3(\omega)v^\lambda v'^\mu + N_4(\omega)g^{\lambda\mu}\Big]\gamma_5 u_{B_b}(v,s),$$

$$M_A^\mu = \langle B_c^*(v',s')|\bar{c}\gamma^\mu\gamma_5 b|B_b(v,s)\rangle$$
$$= \bar{u}_{B_c^*,\lambda}(v',s')\Big[K_1(\omega)v^\lambda\gamma^\mu + K_2(\omega)v^\lambda v^\mu$$
$$+K_3(\omega)v^\lambda v'^\mu + K_4(\omega)g^{\lambda\mu}\Big]u_{B_b}(v,s), \quad (5)$$

where $u_{B_c^*,\lambda}$ is the Rarita–Schwinger spinor for the B_c^* baryon.

Again using equations of motion, the scalar and pseudoscalar matrix elements can be obtained as before and are given by

$$\langle B_c^*(v',s')|\bar{c}b|B_b(v,s)\rangle = \bar{u}_{B_c^*,\lambda}(v',s')\Big[N_1(\omega)v^\lambda \times\frac{\not{q}}{(m_b-m_c)} + N_2(\omega)v^\lambda \times\left(\frac{m_{B_b}^2 - m_{B_c^*}^2 + q^2}{2m_{B_b}(m_b-m_c)}\right) +N_3(\omega)v^\lambda \times\left(\frac{m_{B_b}^2 - m_{B_c^*}^2 - q^2}{2m_{B_c^*}(m_b-m_c)}\right) +N_4(\omega)\frac{q^\lambda}{(m_b-m_c)}\Big] \times\gamma_5 u_{B_b}(v,s),$$

$$\langle B_c^*(v',s')|\bar{c}\gamma_5 b|B_b(v,s)\rangle = \bar{u}_{B_c^*,\lambda}(v',s')\Big[-K_1(\omega)v^\lambda \times\frac{\not{q}}{(m_b+m_c)} - K_2(\omega)v^\lambda \times\left(\frac{m_{B_b}^2 - m_{B_c^*}^2 + q^2}{2m_{B_b}(m_b+m_c)}\right) -K_3(\omega)v^\lambda \times\left(\frac{m_{B_b}^2 - m_{B_c^*}^2 - q^2}{2m_{B_c^*}(m_b+m_c)}\right) -K_4(\omega)\frac{q^\lambda}{(m_b+m_c)}\Big] \times u_{B_b}(v,s). \quad (6)$$

In the heavy quark limit, the form factors for the semileptonic decay of $\Xi_b \to \Xi_c$ (scalar diquark picture) can be expressed as

$$F_1(\omega) = \zeta(\omega) + \left(\frac{\overline{\Lambda}}{2m_b} + \frac{\overline{\Lambda}}{2m_c}\right)\big[2\chi(\omega) + \zeta(\omega)\big],$$
$$G_1(\omega) = \zeta(\omega) + \left(\frac{\overline{\Lambda}}{2m_b} + \frac{\overline{\Lambda}}{2m_c}\right)\left[2\chi(\omega) + \frac{\omega-1}{\omega+1}\zeta(\omega)\right],$$
$$F_2(\omega) = G_2(\omega) = -\frac{\overline{\Lambda}}{2m_c}\frac{2}{\omega+1}\zeta(\omega),$$
$$F_3(\omega) = -G_3(\omega) = -\frac{\overline{\Lambda}}{2m_b}\frac{2}{\omega+1}\zeta(\omega), \quad (7)$$

where the parameter $\overline{\Lambda} = (m_{B_b} - m_b)$ and $\zeta(\omega)$ is the leading order Isgur–Wise (IW) function. The additional function $\chi(\omega)$ arises from the $1/m_b$ correction to the HQET Lagrangian. Near the zero recoil point of the daughter baryon, the functions $\zeta(\omega)$ and $\chi(\omega)$ can be approximated by

$$\zeta(\omega) = 1 - \rho_\zeta^2(\omega-1) + c_\zeta(\omega-1)^2 + \cdots,$$
$$\chi(\omega) = \rho_\chi^2(\omega-1) + c_\chi(\omega-1)^2 + \cdots, \quad (8)$$

where ρ^2 gives the slope and c gives the curvature of the IW functions. The values of these parameters are $\overline{\Lambda}$ (GeV) $= 0.970$, $\rho_\zeta^2 = 2.27$, $c_\zeta = 3.87$, $\rho_\chi^2 = 0.045$ and $c_\chi = 0.036$.

For the semileptonic decays of $\Sigma_b \to \Sigma_c^{(*)}$ (axial-vector diquark picture), the form factors in the heavy quark limit can be expressed in terms of the Isgur–Wise function $\zeta_1(\omega)$ as

$$F_1(\omega) = G_1(\omega) = -\frac{1}{3}\zeta_1(\omega),$$
$$F_2(\omega) = F_3(\omega) = \frac{2}{3}\frac{2}{\omega+1}\zeta_1(\omega),$$
$$G_2(\omega) = G_3(\omega) = 0,$$
$$N_1(\omega) = -N_3(\omega) = K_3(\omega) = -\frac{1}{\sqrt{3}}\frac{2}{\omega+1}\zeta_1(\omega),$$
$$N_4(\omega) = -K_4(\omega) = -\frac{2}{\sqrt{3}}\zeta_1(\omega),$$
$$N_2(\omega) = K_1(\omega) = K_2(\omega) = 0. \quad (9)$$

Again, near the zero recoil point of the daughter baryon, the $\zeta_1(\omega)$ function can be approximated by

$$\zeta_1(\omega) = \zeta_1(1) - \rho_{\zeta_1}^2(\omega-1) + c_{\zeta_1}(\omega-1)^2 + \cdots, \quad (10)$$

where $\rho_{\zeta_1}^2$ gives the slope and c_{ζ_1} gives the curvature of the IW functions. The values of these parameters are $\rho_{\zeta_1}^2 = 2.17$ and $c_{\zeta_1} = 3.62$. Further details of the Isgur–Wise functions used in this work can be found in [47].

2.2 Helicity amplitudes

The helicity amplitudes are defined as [49,56,76,85,86]

$$H^{V,A}_{\lambda_2,\lambda_W} = M^{V,A}_\mu(\lambda_2)\epsilon^{*\mu}(\lambda_W), \quad (11)$$

where λ_2 and λ_W are the helicities of the daughter baryon and the virtual vector boson, respectively; $\epsilon^{*\mu}$ is the polarization vector of the virtual vector boson.

In the parent baryon (B_b) rest frame, the vector (V) and axial vector (A) helicity amplitudes can be obtained in terms

of form factors and NP couplings. The scalar (S) and pseudoscalar (P) helicity amplitudes corresponding to new scalar and pseudoscalar interactions can be obtained using equations of motion.

For $1/2 \to 1/2$ transition, the helicity amplitudes are given by

$$\begin{aligned}
H^{V,A}_{\frac{1}{2},0} &= (1+C_{V_L} \pm C_{V_R})\Bigg\{\frac{1}{\sqrt{q^2}}\sqrt{2m_{B_b}m_{B_c}(\omega \mp 1)} \\
&\quad\times\Bigg[(m_{B_b} \pm m_{B_c})F_1^{V,A}(\omega) \pm m_{B_c}(\omega \pm 1)F_2^{V,A}(\omega) \\
&\quad\pm m_{B_b}(\omega \pm 1)F_3^{V,A}(\omega)\Bigg]\Bigg\}, \\
H^{V,A}_{\frac{1}{2},t} &= (1+C_{V_L} \pm C_{V_R})\Bigg\{\frac{1}{\sqrt{q^2}}\sqrt{2m_{B_b}m_{B_c}(\omega \pm 1)} \\
&\quad\times\Bigg[(m_{B_b} \mp m_{B_c})F_1^{V,A}(\omega) \pm (m_{B_b} - m_{B_c}\omega)F_2^{V,A}(\omega) \\
&\quad\pm(m_{B_b}\omega - m_{B_c})F_3^{V,A}(\omega)\Bigg]\Bigg\}, \\
H^{V,A}_{\frac{1}{2},1} &= (1+C_{V_L} \pm C_{V_R})\Bigg[-2\sqrt{m_{B_b}m_{B_c}(\omega \mp 1)}F_1^{V,A}(\omega)\Bigg], \\
H^{S,P}_{\frac{1}{2},0} &= (C_{S_L} \pm C_{S_R})\Bigg\{\frac{\sqrt{2m_{B_b}m_{B_c}(\omega \pm 1)}}{m_b \mp m_c} \\
&\quad\times\Bigg[(m_{B_b} \mp m_{B_c})F_1^{V,A}(\omega) \\
&\quad\pm\left(\frac{m^2_{B_b} - m^2_{B_c} + q^2}{2m_{B_b}}\right)F_2^{V,A}(\omega) \\
&\quad\pm\left(\frac{m^2_{B_b} - m^2_{B_c} - q^2}{2m_{B_c}}\right)F_3^{V,A}(\omega)\Bigg]\Bigg\}. \qquad (12)
\end{aligned}$$

For $1/2 \to 3/2$ transition, the helicity amplitudes are given by

$$\begin{aligned}
H^{V,A}_{\frac{1}{2},0} &= (1+C_{V_L} \pm C_{V_R})\Bigg\{\mp\frac{1}{\sqrt{q^2}}\frac{2}{\sqrt{3}}\sqrt{m_{B_b}m_{B^*_c}(\omega \mp 1)} \\
&\quad\times\Bigg[\mp(m_{B_b} \mp m_{B^*_c})(\omega \pm 1)N_1^{V,A}(\omega) \\
&\quad+ m_{B^*_c}(\omega^2-1)N_2^{V,A}(\omega) + m_{B_b}(\omega^2-1)N_3^{V,A}(\omega) \\
&\quad+(m_{B_b}\omega - m_{B^*_c})N_4^{V,A}(\omega)\Bigg]\Bigg\}, \\
H^{V,A}_{\frac{1}{2},t} &= (1+C_{V_L} \pm C_{V_R})\Bigg\{\mp\frac{1}{\sqrt{q^2}}\frac{2}{\sqrt{3}}\sqrt{m_{B_b}m_{B^*_c}(\omega \pm 1)} \\
&\quad\times(\omega \mp 1)\Bigg[\mp(m_{B_b} \pm m_{B^*_c})N_1^{V,A}(\omega) \\
&\quad+(m_{B_b} - m_{B^*_c}\omega)N_2^{V,A}(\omega) \\
&\quad+(m_{B_b}\omega - m_{B^*_c})N_3^{V,A}(\omega) + m_{B_b}N_4^{V,A}(\omega)\Bigg]\Bigg\}, \\
H^{V,A}_{\frac{1}{2},1} &= (1+C_{V_L} \pm C_{V_R})\sqrt{\frac{2}{3}}\sqrt{m_{B_b}m_{B^*_c}(\omega \mp 1)} \\
&\quad\times\Bigg[-2(\omega \pm 1)N_1^{V,A}(\omega) + N_4^{V,A}(\omega)\Bigg], \\
H^{V,A}_{\frac{3}{2},1} &= (1+C_{V_L} \pm C_{V_R})\Bigg[\mp\sqrt{2m_{B_b}m_{B^*_c}(\omega \mp 1)}N_4^{V,A}(\omega)\Bigg],
\end{aligned}$$

$$\begin{aligned}
H^{S,P}_{\frac{1}{2},0} &= (C_{S_L} \pm C_{S_R})\Bigg\{-\sqrt{\frac{2}{3}}\frac{\sqrt{2m_{B_b}m_{B^*_c}(\omega \pm 1)}}{(m_b \mp m_c)} \\
&\quad\times\frac{2m_{B_b}m_{B^*_c}(\omega \mp 1)}{2m_{B^*_c}}\Bigg[\mp\left(\frac{m_{B_b} \pm m_{B^*_c}}{m_{B_b}}\right)N_1^{V,A}(\omega) \\
&\quad+\left(\frac{m^2_{B_b} - m^2_{B^*_c} + q^2}{2m^2_{B_b}}\right)N_2^{V,A}(\omega) \\
&\quad+\left(\frac{m^2_{B_b} - m^2_{B^*_c} - q^2}{2m_{B_b}2m_{B^*_c}}\right)N_3^{V,A}(\omega) + N_4^{V,A}(\omega)\Bigg]\Bigg\}. \qquad (13)
\end{aligned}$$

The remaining helicity amplitudes can be obtained using parity relations

$$\begin{aligned}
H^{V,A}_{-\lambda_2,-\lambda_W} &= \pm H^{V,A}_{\lambda_2,\lambda_W} \quad (1/2^+ \to 1/2^+) \\
H^{V,A}_{-\lambda_2,-\lambda_W} &= \mp H^{V,A}_{\lambda_2,\lambda_W} \quad (1/2^+ \to 3/2^+) \\
H^{S,P}_{-\lambda_2,-\lambda_{\rm NP}} &= \pm H^{S,P}_{\lambda_2,\lambda_{\rm NP}} \quad (1/2^+ \to 1/2^+) \\
H^{S,P}_{-\lambda_2,-\lambda_{\rm NP}} &= \mp H^{S,P}_{\lambda_2,\lambda_{\rm NP}} \quad (1/2^+ \to 3/2^+)\,. \qquad (14)
\end{aligned}$$

The total helicity amplitudes are given by

$$\begin{aligned}
H_{\lambda_2,\lambda_W} &= H^V_{\lambda_2,\lambda_W} - H^A_{\lambda_2,\lambda_W} \\
H^{SP}_{\lambda_2,0} &= H^S_{\lambda_2,0} - H^P_{\lambda_2,0}\,. \qquad (15)
\end{aligned}$$

2.3 q^2-dependent observables

The twofold angular distribution for the $B_b \to B_c^{(*)}\ell^-\bar{\nu}_\ell$ decay including NP contributions can be written as [49]

$$\begin{aligned}
\frac{d^2\Gamma}{dq^2 d\cos\theta_\ell} &= \frac{G_F^2|V_{cb}|^2 q^2 |\mathbf{p}_{B_c^{(*)}}|}{512\pi^3 m^2_{B_1}}\left(1-\frac{m^2_\ell}{q^2}\right)^2 \\
&\quad\times\left[A_1 + \frac{m^2_\ell}{q^2}A_2 + 2A_3 + \frac{4m_\ell}{\sqrt{q^2}}A_4\right], \qquad (16)
\end{aligned}$$

where θ_ℓ is the angle of the lepton with respect to the W momentum in the rest frame of the W boson, $|\mathbf{p}_{B_c^{(*)}}| = \frac{\sqrt{\lambda(m^2_{B_b}, m^2_{B_c^{(*)}}, q^2)}}{2m_{B_b}}$, and

$$\begin{aligned}
A_1 &= 2\sin^2\theta_\ell\left(H^2_{\frac{1}{2},0} + H^2_{-\frac{1}{2},0}\right) + (1-\cos\theta_\ell)^2\Big(H^2_{\frac{1}{2},1} \\
&\quad+H^2_{\frac{3}{2},1}\Big) + (1+\cos\theta_\ell)^2\left(H^2_{-\frac{1}{2},-1} + H^2_{-\frac{3}{2},-1}\right), \\
A_2 &= 2\cos^2\theta_\ell\left(H^2_{\frac{1}{2},0} + H^2_{-\frac{1}{2},0}\right) + \sin^2\theta_\ell\Big(H^2_{\frac{1}{2},1} + H^2_{-\frac{1}{2},-1} \\
&\quad+H^2_{\frac{3}{2},1} + H^2_{-\frac{3}{2},-1}\Big) + 2\left(H^2_{\frac{1}{2},t} + H^2_{-\frac{1}{2},t}\right) \\
&\quad-4\cos\theta_\ell\left(H_{\frac{1}{2},t}H_{\frac{1}{2},0} + H_{-\frac{1}{2},t}H_{-\frac{1}{2},0}\right), \\
A_3 &= \left(H^{SP}_{\frac{1}{2},0}\right)^2 + \left(H^{SP}_{-\frac{1}{2},0}\right)^2, \\
A_4 &= -\cos\theta_\ell\left(H_{\frac{1}{2},0}H^{SP}_{\frac{1}{2},0} + H_{-\frac{1}{2},0}H^{SP}_{-\frac{1}{2},0}\right) \\
&\quad+\left(H_{\frac{1}{2},t}H^{SP}_{\frac{1}{2},0} + H_{-\frac{1}{2},t}H^{SP}_{-\frac{1}{2},0}\right). \qquad (17)
\end{aligned}$$

Table 1 Form factors predictions for $\Lambda_b \to \Lambda_c$ at $q^2 = 0$ and $q^2 = q^2_{max}$

	$f_+(0)$	$f_\perp(0)$	$f_0(0)$	$g_+(0)$	$g_\perp(0)$	$g_0(0)$
RQM [47]	0.796	1.013	0.796	0.796	0.783	0.796
LQCD [41]	0.418	0.558	0.416	0.377	0.375	0.378
	$f_+(q^2_{max})$	$f_\perp(q^2_{max})$	$f_0(q^2_{max})$	$g_+(q^2_{max})$	$g_\perp(q^2_{max})$	$g_0(q^2_{max})$
RQM [47]	1.088	1.392	0.999	0.999	0.999	1.088
LQCD [41]	1.126	1.491	0.986	0.903	0.903	1.030

The helicity amplitude squared terms $\left(H^2_{\frac{3}{2},1}\right)$ and $\left(H^2_{-\frac{3}{2},-1}\right)$ contribute only to the $B_b \to B_c^* \ell^- \bar{\nu}_\ell$ case.

On integrating out $\cos\theta_\ell$ from Eq. (16), the differential decay rate for the $B_b \to B_c^{(*)} \ell^- \bar{\nu}_\ell$ decay including NP contributions can be obtained as

$$\frac{d\Gamma}{dq^2} = \frac{G_F^2 |V_{cb}|^2 q^2 |\mathbf{p}_{B_c^{(*)}}|}{192\pi^3 m_{B_b}^2} \left(1 - \frac{m_\ell^2}{q^2}\right)^2 H_{\frac{1}{2}\to\frac{1}{2}\left(\frac{3}{2}\right)}, \tag{18}$$

where

$$\begin{aligned} H_{\frac{1}{2}\to\frac{1}{2}} &= \left(H^2_{\frac{1}{2}0}\right) + \left(H^2_{-\frac{1}{2}0}\right) + \left(H^2_{\frac{1}{2}1}\right) + \left(H^2_{-\frac{1}{2}-1}\right) \\ &+ \frac{m_\ell^2}{2q^2}\Big[\left(H^2_{\frac{1}{2}0}\right) + \left(H^2_{-\frac{1}{2}0}\right) + \left(H^2_{\frac{1}{2}1}\right) + \left(H^2_{-\frac{1}{2}-1}\right) \\ &+ 3\left(H^2_{\frac{1}{2}t} + H^2_{-\frac{1}{2}t}\right)\Big] + \frac{3}{2}\left[\left(H^{SP}_{\frac{1}{2}0}\right)^2 + \left(H^{SP}_{-\frac{1}{2}0}\right)^2\right] \\ &+ \frac{3m_\ell}{\sqrt{q^2}}\left[H_{\frac{1}{2}t} H^{SP}_{\frac{1}{2}0} + H_{-\frac{1}{2}t} H^{SP}_{-\frac{1}{2}0}\right] \end{aligned} \tag{19}$$

and

$$\begin{aligned} H_{\frac{1}{2}\to\frac{3}{2}} &= \left(H^2_{\frac{1}{2}0}\right) + \left(H^2_{-\frac{1}{2}0}\right) + \left(H^2_{\frac{1}{2}1}\right) + \left(H^2_{-\frac{1}{2}-1}\right) \\ &+ \left(H^2_{\frac{3}{2}1}\right) + \left(H^2_{-\frac{3}{2}-1}\right) + \frac{m_\ell^2}{2q^2}\Big[\left(H^2_{\frac{1}{2}0}\right) + \left(H^2_{-\frac{1}{2}0}\right) \\ &+ \left(H^2_{\frac{1}{2}1}\right) + \left(H^2_{-\frac{1}{2}-1}\right) + \left(H^2_{\frac{3}{2}1}\right) + \left(H^2_{-\frac{3}{2}-1}\right) \\ &+ 3\left(H^2_{\frac{1}{2}t} + H^2_{-\frac{1}{2}t}\right)\Big] + \frac{3}{2}\left[\left(H^{SP}_{\frac{1}{2}0}\right)^2 + \left(H^{SP}_{-\frac{1}{2}0}\right)^2\right] \\ &+ \frac{3m_\ell}{\sqrt{q^2}}\left[H_{\frac{1}{2}t} H^{SP}_{\frac{1}{2}0} + H_{-\frac{1}{2}t} H^{SP}_{-\frac{1}{2}0}\right]. \end{aligned} \tag{20}$$

The differential branching fraction is given by

$$DBR(q^2) = \tau_{B_b}\left(\frac{d\Gamma}{dq^2}\right). \tag{21}$$

Apart from these, other interesting q^2-dependent observables are defined, such as:

Ratio of branching fractions

$$R_{B_c^{(*)}}(q^2) = \frac{\frac{d\Gamma}{dq^2}(B_b \to B_c^{(*)} \tau^- \bar{\nu}_\tau)}{\frac{d\Gamma}{dq^2}(B_b \to B_c^{(*)} \ell^- \bar{\nu}_\ell)}, \tag{22}$$

Forward-backward asymmetry of the charged lepton

$$A^\tau_{FB}(q^2) = \frac{\left(\int_0^1 - \int_{-1}^0\right) \frac{d^2\Gamma}{dq^2 d\cos\theta_\ell} d\cos\theta_\ell}{\left(\int_0^1 + \int_{-1}^0\right) \frac{d^2\Gamma}{dq^2 d\cos\theta_\ell} d\cos\theta_\ell}, \tag{23}$$

Convexity parameter

$$C^\tau_F(q^2) = \frac{1}{d\Gamma/dq^2} \frac{d^2}{d(\cos\theta_\ell)^2}\left(\frac{d^2\Gamma}{dq^2 d\cos\theta_\ell}\right), \tag{24}$$

Longitudinal polarization of the charged lepton

$$P^\tau_L(q^2) = \frac{\frac{d\Gamma^{\lambda_\tau=1/2}}{dq^2} - \frac{d\Gamma^{\lambda_\tau=-1/2}}{dq^2}}{\frac{d\Gamma^{\lambda_\tau=1/2}}{dq^2} + \frac{d\Gamma^{\lambda_\tau=-1/2}}{dq^2}}, \tag{25}$$

where $d\Gamma^{\lambda_\tau=\pm 1/2}/dq^2$ are helicity-dependent differential decay rates.

3 Comparison of RQM and LQCD predictions

In this section, we first confront the theoretical predictions obtained in the relativistic quark model framework [47] with those obtained using lattice QCD [41]. Since lattice results are available for the well-studied mode $\Lambda_b \to \Lambda_c \tau^- \bar{\nu}_\tau$, we therefore present the comparison for form factors calculated in RQM and in LQCD for the semileptonic Λ_b to Λ_c decay at $q^2 = 0$ and $q^2 = q^2_{max}$ in Table 1. Such a comparison can help to comprehend the different approaches used in the determination of form factors for baryons. From Table 1, it can be seen that the RQM form factor predictions and those from lattice results are in reasonable agreement at the zero recoil point of the daughter baryon. This is observed in the

Table 2 Theoretical predictions for $\Lambda_b \to \Lambda_c \tau^- \bar{\nu}_\tau$

	RQM [47]	ELA [50]	LQCD [41]
$\Gamma/\lvert V_{cb}\rvert^2$ ps^{-1}	9.91 ± 0.29		$7.15 \pm 0.15 \pm 0.27$
$Br(\%)$	2.43	1.63	
R_{Λ_c}	0.25	0.3379	$0.3328 \pm 0.0074 \pm 0.0070$

case of b-meson decays [87] also. The relation between the RQM form factors and those used in lattice calculations are given in Appendix A.

In the RQM framework, the uncertainties coming from the form factors were estimated to be not more than 5% [48,88]. These uncertainties were shown to have their origin in the uncertainties of the baryon wave functions used in the calculation of the form factors. Using RQM form factors and considering a 5% uncertainty coming from the form factor inputs, we find that the predicted total decay rate divided by the square of the CKM matrix element is $\Gamma(\Lambda_b \to \Lambda_c \tau^- \bar{\nu}_\tau)/|V_{cb}|^2 = (9.91 \pm 0.29)$ ps^{-1} and the relative error is 2.9%. With lattice form factors, the prediction is $\Gamma(\Lambda_b \to \Lambda_c \tau^- \bar{\nu}_\tau)/|V_{cb}|^2 = (7.15 \pm 0.15 \pm 0.27)$ ps^{-1}. Here, the relative error is about 2%. When the branching ratio is compared, we find that the prediction using lattice form factors within an effective Lagrangian approach (ELA) [50] is smaller compared to that obtained using RQM. Predictions for the ratio $R_{\Lambda_c} = Br(\Lambda_b \to \Lambda_c \tau^- \bar{\nu}_\tau)/Br(\Lambda_b \to \Lambda_c \ell^- \bar{\nu}_\ell)$ in RQM are somewhat smaller compared to lattice predictions. However, it should be noted that the sensitivity of these ratios to form factor uncertainties is less as these cancel out partially in these ratios. The predictions compared here are presented in Table 2.

In Fig. 1, we also display the differential branching fraction prediction for $\Lambda_b \to \Lambda_c \tau^- \bar{\nu}_\tau$ decay with RQM and LQCD calculations within the SM. It can be observed that there is a sizeable difference in the differential distribution and this may be attributed to the variation in the q^2-dependence of the form factors. However, close to the point of zero recoil, the two predictions are in agreement with each other.

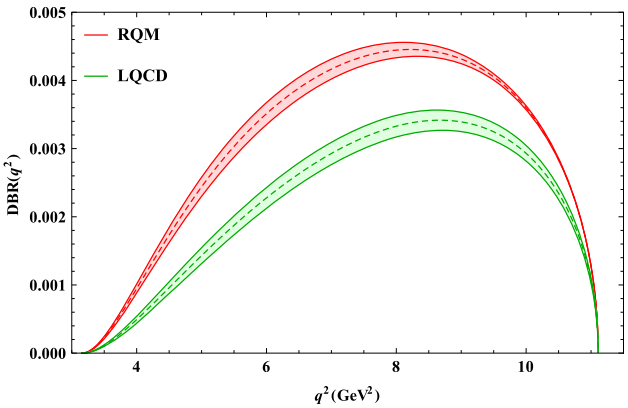

Fig. 1 Comparison of the differential branching fraction for $\Lambda_b \to \Lambda_c \tau^- \bar{\nu}_\tau$ decay in the SM obtained using RQM framework (red) and lattice calculations (green)

4 New physics sensitivity

We now proceed to study the NP sensitivity of the various q^2-dependent observables defined in the earlier section for the modes $\Xi_b \to \Xi_c \tau^- \bar{\nu}_\tau$ and $\Sigma_b \to \Sigma_c^{(*)} \tau^- \bar{\nu}_\tau$. The input parameters used for our numerical analysis are listed in Table 3.

For the SM calculation of decay amplitudes, the theoretical uncertainties that arise from the input parameters such as the CKM matrix element V_{cb} and the form factors are taken into consideration. We consider the V_{cb} uncertainty as given in Table 3 and a 5% uncertainty coming from the form factor inputs as determined in [48,88]. We constrain the new couplings $C_{V_L}, C_{S_L}, C_{S_R}$ using the experimental measurements of $R_{D^{(*)}}$, $R_{J/\psi}$, $F_L^{D^*}$ and $P_\tau^{D^*}$. A 30% constraint is also imposed from the upper bound of $\mathcal{B}(B_c^+ \to \tau^+ \nu_\tau)$ [90]. The relevant relations pertaining to these observables are given below.

The differential decay rate of $\bar{B} \to D \tau^- \bar{\nu}_\tau$ is given by [19]

$$\begin{aligned}\frac{d\Gamma(\bar{B} \to D\tau^-\bar{\nu}_\tau)}{dq^2} &= \frac{G_F^2 |V_{cb}|^2}{192\pi^3 m_B^3} q^2 \sqrt{\lambda_D(q^2)} \left(1 - \frac{m_\tau^2}{q^2}\right)^2 \\ &\times \Bigg\{ |1 + C_{V_L} + C_{V_R}|^2 \Bigg[\left(1 + \frac{m_\tau^2}{2q^2}\right) \\ &\times H_{V,0}^2 + \frac{3}{2} \frac{m_\tau^2}{q^2} H_{V,t}^2 \Bigg] \\ &+ \frac{3}{2} |C_{S_R} + C_{S_L}|^2 H_S^2 \\ &+ 3Re\Big[\big(1 + C_{V_L} + C_{V_R}\big) \big(C_{S_R}^* \\ &+ C_{S_L}^*\big) \Big] \frac{m_\tau}{\sqrt{q^2}} H_S H_{V,t} \Bigg\}, \end{aligned} \tag{26}$$

where the hadronic helicity amplitudes $H_{V,0}$, $H_{V,t}$ and H_S are expressed in terms of the Caprini et al. parametrized HQET form factors [91]. These form factors are evaluated using parameters obtained from lattice QCD calculations [92].

Table 3 Input parameters [89]

$G_F = 1.166378 \times 10^{-5}$ GeV^{-2}	$m_{\Xi_b} = 5.7970$ GeV
$V_{cb} = (41.0 \pm 1.4) \times 10^{-3}$	$m_{\Xi_c} = 2.47090$ GeV
$m_\tau = 1.77686$ GeV	$m_{\Sigma_b} = 5.81564$ GeV
$m_\mu = 0.105658$ GeV	$m_{\Sigma_c} = 2.45375$ GeV
$m_b = 4.18$ GeV	$m_{\Sigma_c^*} = 2.51848$ GeV
$m_c = 1.27$ GeV	$\tau_{\Xi_b} = 1.572$ ps
$m_e = 0.00051099$ GeV	

The differential decay rate of $\bar{B} \to D^* \tau^- \bar{\nu}_\tau$ is given by [19,93]

$$\begin{aligned}\frac{d\Gamma(\bar{B} \to D^* \tau^- \bar{\nu}_\tau)}{dq^2} &= \frac{G_F^2 |V_{cb}|^2}{192\pi^3 m_B^3} q^2 \sqrt{\lambda_{D^*}(q^2)} \left(1 - \frac{m_\tau^2}{q^2}\right)^2 \\ &\times \Bigg\{ (|1 + C_{V_L}|^2 + |C_{V_R}|^2) \\ &\times \Bigg[\left(1 + \frac{m_\tau^2}{2q^2}\right) \left(H_{V,0}^2 + H_{V,+}^2 \right. \\ &\left. + H_{V,-}^2\right) + \frac{3}{2} \frac{m_\tau^2}{q^2} H_{V,t}^2 \Bigg] \\ &- 2Re\left[\left(1 + C_{V_L}\right) C_{V_R}^*\right] \\ &\times \Bigg[\left(1 + \frac{m_\tau^2}{2q^2}\right) \left(H_{V,0}^2 \right. \\ &\left. + 2H_{V,+} H_{V,-}\right) + \frac{3}{2} \frac{m_\tau^2}{q^2} H_{V,t}^2 \Bigg] \\ &+ \frac{3}{2} |C_{S_R} - C_{S_L}|^2 H_S^2 \\ &+ 3Re\Big[\left(1 + C_{V_L} - C_{V_R}\right)\left(C_{S_R}^* \right. \\ &\left. - C_{S_L}^*\right)\Big] \frac{m_\tau}{\sqrt{q^2}} H_S H_{V,t} \Bigg\}, \end{aligned} \tag{27}$$

where $H_{V,0}$, $H_{V,\pm}$, $H_{V,t}$ and H_S are the hadronic helicity amplitudes. Here $\lambda_{D^{(*)}}(q^2) = [(m_B - m_{D^{(*)}})^2 - q^2][(m_B + m_{D^{(*)}})^2 - q^2]$.

We use $\bar{B} \to D^*$ HQET form factors parametrized by Caprini et al. [91] where the fitted parameters are determined by HFLAV [1]. The differential decay rate expression for $B_c \to J/\psi \tau^- \bar{\nu}_\tau$ is similar to that of $\bar{B} \to D^* \tau^- \bar{\nu}_\tau$ with appropriate substitutions for masses and form factors. For this mode, we use the form factors obtained in [93,94] by employing perturbative QCD approach.

The longitudinal polarization of τ ($P_\tau^{D^*}$) and of D^* ($F_L^{D^*}$) in $B \to D^* \tau^- \bar{\nu}_\tau$ are respectively given by

$$P_\tau^{D^*} = \frac{\Gamma(\lambda_\tau = 1/2) - \Gamma(\lambda_\tau = -1/2)}{\Gamma(\lambda_\tau = 1/2) + \Gamma(\lambda_\tau = -1/2)}, \tag{28}$$

$$F_L^{D^*} = \frac{\Gamma_{\lambda_{D^*}=0}(B \to D^* \tau^- \bar{\nu}_\tau)}{\Gamma(B \to D^* \tau^- \bar{\nu}_\tau)}, \tag{29}$$

Table 4 Experimental and theoretical values of $R_{D^{(*)}}$, $R_{J\psi}$, $F_L^{D^*}$, $P_\tau^{D^*}$

Observable	Experimental value	SM value
R_D	$0.339 \pm 0.026 \pm 0.014$	0.299 ± 0.003
R_{D^*}	$0.295 \pm 0.010 \pm 0.010$	0.254 ± 0.005
$R_{J/\psi}$	$0.71 \pm 0.17 \pm 0.18$	0.289 ± 0.01
$F_L^{D^*}$	$0.60 \pm 0.08 \pm 0.04$	0.457 ± 0.010
$P_\tau^{D^*}$	$-0.38 \pm 0.51^{+0.21}_{-0.16}$	-0.497 ± 0.013

Table 5 Best-fit values of the NP couplings

NP coupling	Best-fit value	1σ range
C_{V_L}	0.0750	[0.0567, 0.0929]
C_{S_L}	0.1147	[0.0672, 0.1591]
C_{S_R}	0.1323	[0.0906, 0.1719]

where λ_τ and λ_{D^*} denote the helicity of τ and D^*, respectively.

The branching fraction of $B_c^+ \to \tau^+ \nu_\tau$ is given by

$$\begin{aligned}\mathcal{B}(B_c^+ \to \tau^+ \nu_\tau) &= \frac{G_F^2 |V_{cb}|^2 m_\tau^2}{8\pi} \tau_{B_c} m_{B_c} f_{B_c}^2 \left(1 - \frac{m_\tau^2}{m_{B_c}^2}\right)^2 \\ &\times \left| (1 + C_{V_L} - C_{V_R}) - \frac{m_{B_c}^2}{m_\tau (m_b + m_c)} \right. \\ &\left. \times (C_{S_R} - C_{S_L}) \right|^2. \end{aligned} \tag{30}$$

We use $f_{B_c} = 489 \pm 4 \pm 3$MeV from [95] and the values of other constants are taken from [89].

In our work, we consider one new coupling at a time and the best-fit values are obtained by performing a χ^2 fitting. The χ^2 function is defined as

$$\chi^2(C_k) = \sum_{ij}^{N_{obs}} [O_i^{exp} - O_i^{th}(C_k)] \mathcal{C}_{ij}^{-1} [O_j^{exp} - O_j^{th}(C_k)], \tag{31}$$

where O_i^{exp} are the experimental values of the observables, $O_i^{th}(C_k)$ are the theoretical predictions for the observables with new couplings C_k, and $\mathcal{C}$ is the covariance matrix which takes into account the correlation of R_D and R_{D^*}. The χ^2 function is minimized to obtain the best-fit values for each NP coupling. The NP effects are obtained by imposing a 1σ constraint from the measured values of $R_{D^{(*)}}$, $R_{J/\psi}$, $F_L^{D^*}$ and $P_\tau^{D^*}$. The experimental and SM theoretical values of the observables used for obtaining the constraints are listed in Table 4. The obtained best-fit values are listed in Table 5.

The q^2-spectra of various observables for the $\Xi_b \to \Xi_c \tau^- \bar{\nu}_\tau$ and $\Sigma_b \to \Sigma_c^{(*)} \tau^- \bar{\nu}_\tau$ decay modes in the SM case and in the presence of the NP couplings C_{V_L}, C_{S_L}, C_{S_R}

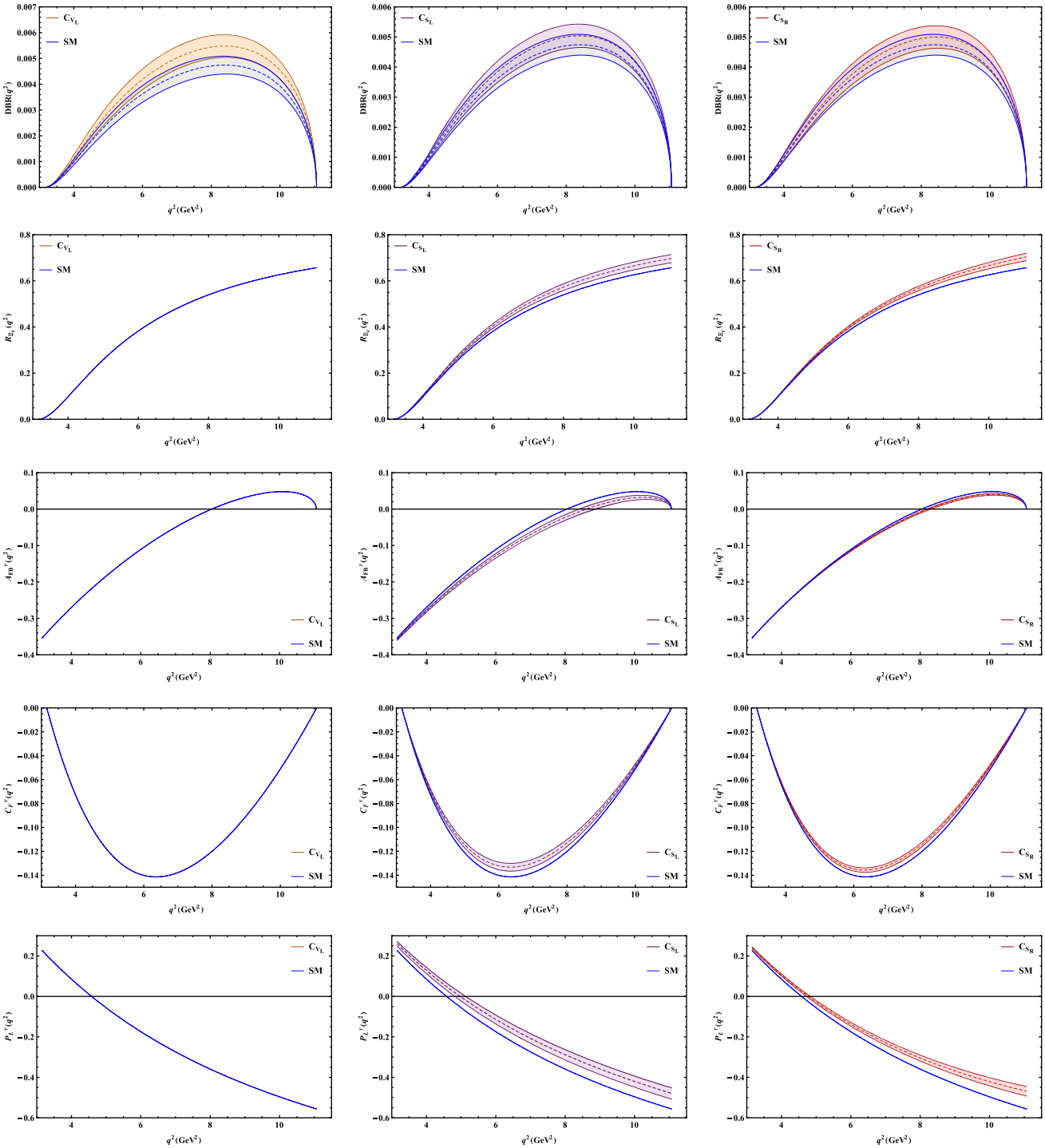

Fig. 2 The q^2-dependence of various observables for the $\Xi_b \to \Xi_c \tau^- \bar{\nu}_\tau$ decay mode in the presence of vector (C_{V_L}) and scalar (C_{S_L}, C_{S_R}) NP couplings

are presented in Figs. 2, 3 and 4. The predictions are distinguished by blue (SM), orange (C_{V_L}), purple (C_{S_L}) and red (C_{S_R}) colors, respectively. For the mode $\Xi_b \to \Xi_c \tau^- \bar{\nu}_\tau$, the differential branching ratio DBR deviates more noticeably from the SM in the presence of the C_{V_L} coupling than in the case with the scalar couplings. The differential decay rate $d\Gamma/dq^2$ is enhanced over the whole q^2 region in the presence of both the vector and scalar couplings for $\Sigma_b \to \Sigma_c \tau^- \bar{\nu}_\tau$ decays. For $\Sigma_b \to \Sigma_c^* \tau^- \bar{\nu}_\tau$ decay mode, $d\Gamma/dq^2$ is enhanced with respect to the vector coupling but is largely unaffected by the scalar couplings. In the case of

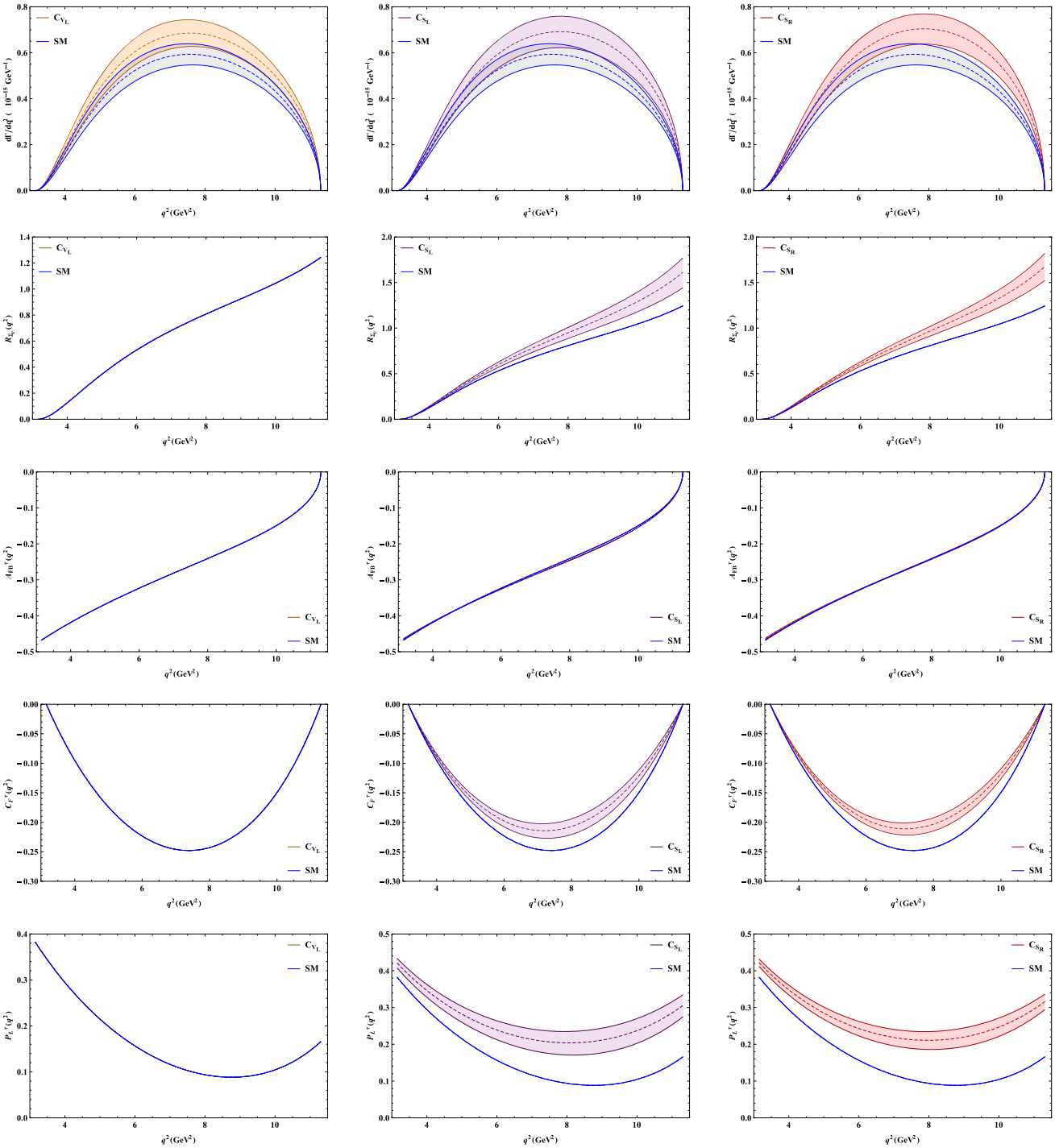

Fig. 3 The q^2-dependence of various observables for the $\Sigma_b \to \Sigma_c \tau^- \bar{\nu}_\tau$ decay mode in the presence of vector (C_{V_L}) and scalar (C_{S_L}, C_{S_R}) NP couplings

the C_{V_L} coupling, the ratio $R_{B_c^{(*)}}$ and all the other observables behave SM-like for all three decay modes, as the NP-dependent factor, $(1 + C_{V_L})^2$ cancels out in these quantities. $R_{\Xi_c(\Sigma_c)}$ displays a distinctive deviation from the SM prediction in the higher q^2 region for C_{S_L} and C_{S_R} couplings. Measuring $R_{\Xi_c(\Sigma_c)}$ in the higher q^2 region may thus further substantiate the observed anomalies in b-decays. No sizable deviation is observed for $R_{\Sigma_c^*}$ in the presence of scalar couplings. The forward-backward asymmetry A_{FB}^{τ} has a SM zero-crossing point at $q^2 \approx 8\,\mathrm{GeV}^2$ for $\Xi_b \to \Xi_c \tau^- \bar{\nu}_\tau$. This shifts to a slightly higher q^2 value in the presence of scalar couplings. For $\Sigma_b \to \Sigma_c \tau^- \bar{\nu}_\tau$, A_{FB}^{τ} reaches 0 at $q^2 \approx q^2_{max}$.

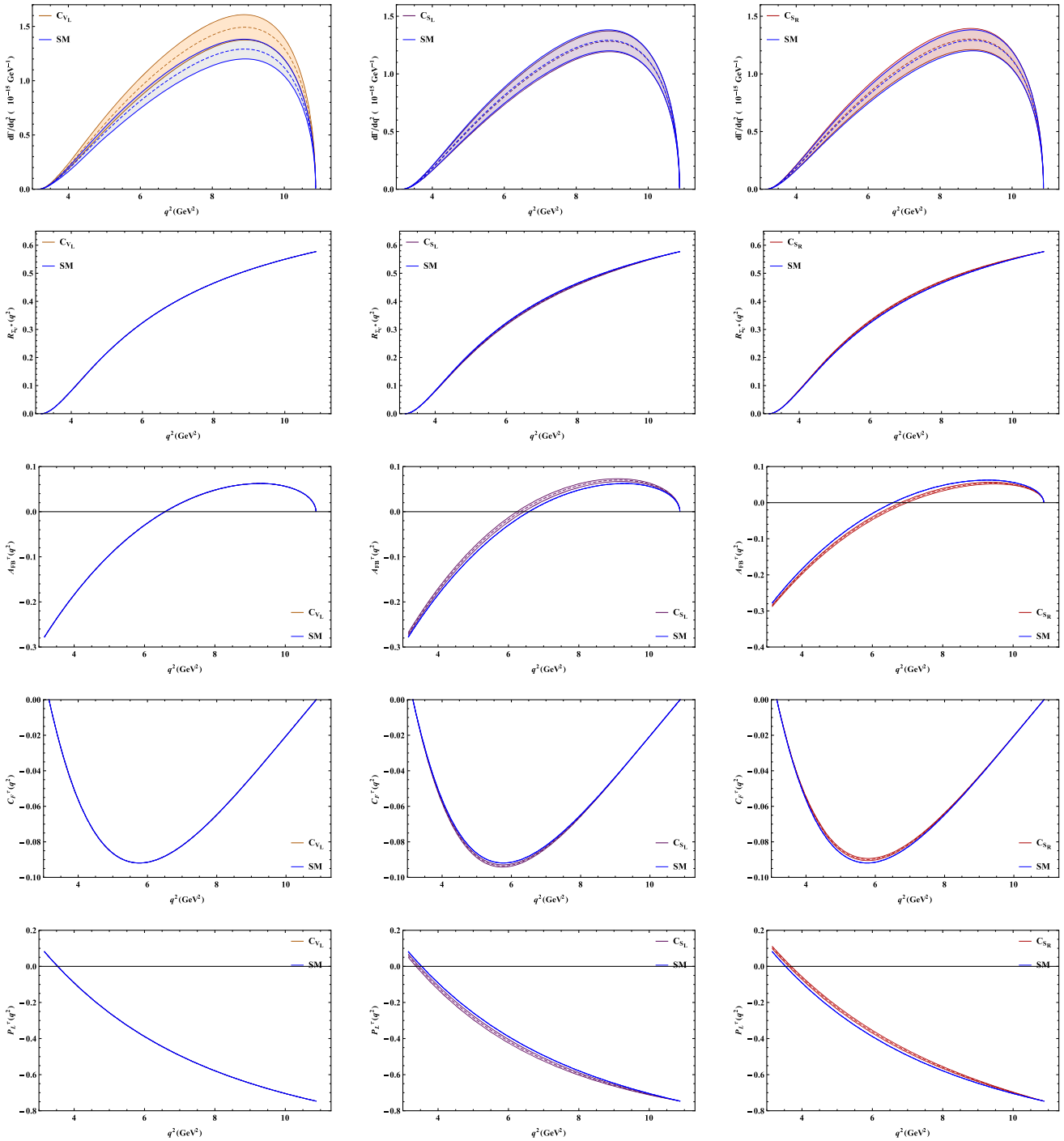

Fig. 4 The q^2-dependence of various observables for the $\Sigma_b \to \Sigma_c^* \tau^- \bar{\nu}_\tau$ decay mode in the presence of vector (C_{V_L}) and scalar (C_{S_L}, C_{S_R}) NP couplings

There is no significant deviation from the SM prediction in the presence of scalar couplings. For the $\Sigma_b \to \Sigma_c^* \tau^- \bar{\nu}_\tau$ decay mode, A_{FB}^{τ} has a SM zero-crossing point at $q^2 \approx 6.6$ GeV^2. The zero-crossing shifts slightly to a lower q^2 value with C_{S_L} coupling and to a higher q^2 value with C_{S_R} coupling. The convexity parameter C_F^{τ} displays a distinctive deviation from the SM prediction in case of C_{S_L} and C_{S_R} couplings for the decay modes considered, with a more pronounced deviation in the case of the $\Sigma_b \to \Sigma_c \tau^- \bar{\nu}_\tau$ mode. The measurement of this observable may further endorse existence of NP beyond the SM. The longitudinal polarization $P_L^{\tau}(q^2)$ has a zero-crossing at $q^2 \approx 4.6$ GeV^2 in the SM

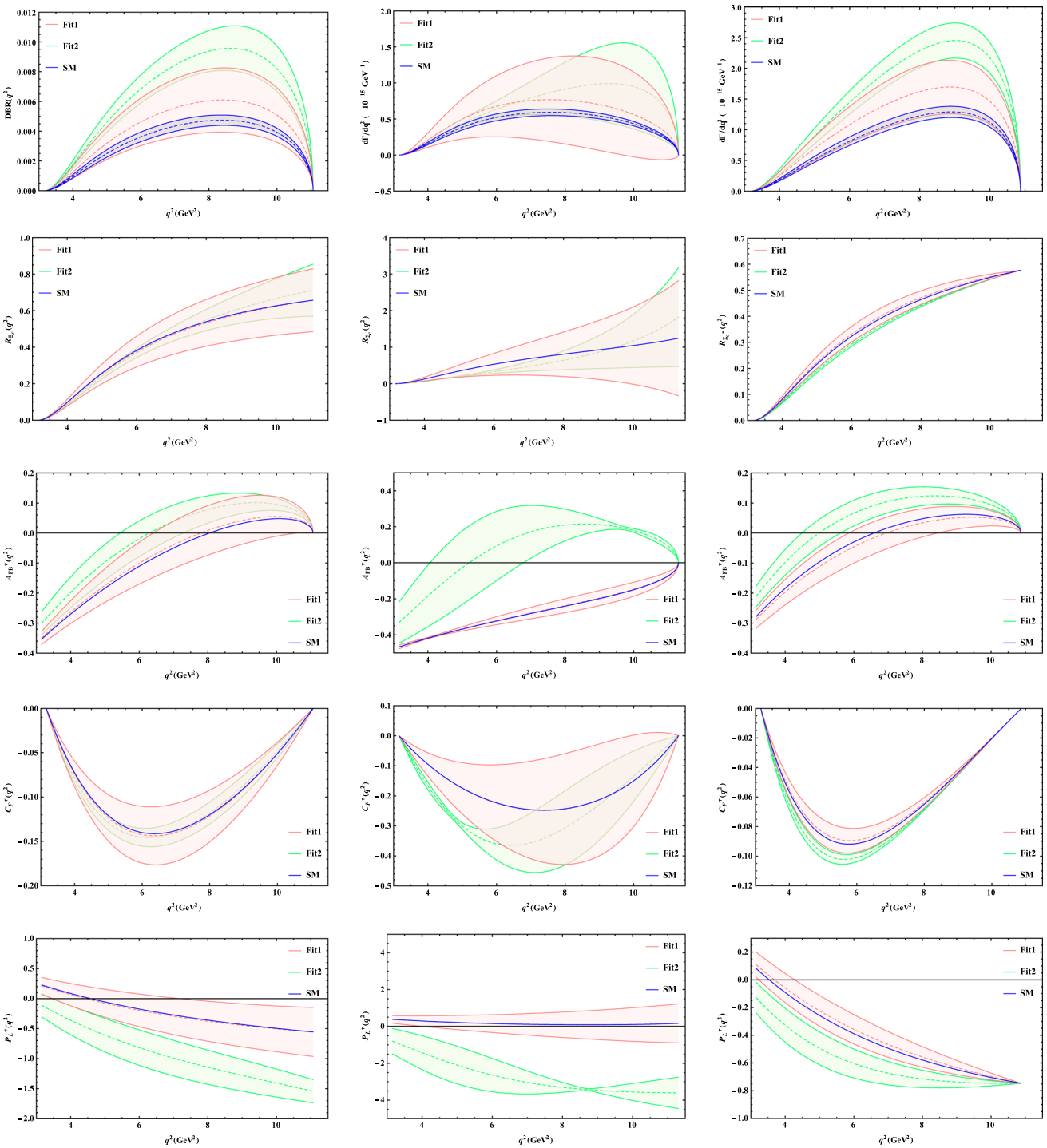

Fig. 5 SM and NP predictions of various q^2-dependent observables for the $\Xi_b \to \Xi_c \tau^- \bar{\nu}_\tau$ (left panel), $\Sigma_b \to \Sigma_c \tau^- \bar{\nu}_\tau$ (central panel) and $\Sigma_b \to \Sigma_c^* \tau^- \bar{\nu}_\tau$ (right panel) decay modes using Fits 1 and 2 of [54]

for $\Xi_b \to \Xi_c \tau^- \bar{\nu}_\tau$ decay. It shifts to a higher q^2 value in case of both the scalar couplings. The deviation from the SM prediction is more prominent at large q^2. For $\Sigma_b \to \Sigma_c \tau^- \bar{\nu}_\tau$ decay, $P_L^\tau(q^2)$ shows a distinct deviation from the SM prediction in the case of the scalar couplings. Thus, measuring $P_L^\tau(q^2)$ may provide insight into the nature of NP and distinguish between the vector and scalar type contributions. For $\Sigma_b \to \Sigma_c^* \tau^- \bar{\nu}_\tau$, a SM zero-crossing point is observed at $q^2 \approx 3.5\ \mathrm{GeV}^2$. This shifts slightly to a lower q^2 value for C_{S_L} coupling and to a higher q^2 value for C_{S_R} coupling.

In addition to our results, we also present the NP predictions obtained using the Wilson coefficients from the global fits (Fits 1 and 2) of Murgui et al. [54] for all three decay modes in Fig. 5. Performing a global χ^2 fit to the data available in $b \to c\tau^-\bar{\nu}_\tau$ transitions, the authors of [54] obtained three fits, Fit 1, 2 and 3, where the coefficient C_{V_R} was assumed to be lepton-flavour universal also. The experimental measurements of the ratios R_D, R_{D^*} and $F_L^{D^*}$ were used to constrain the new couplings. An upper bound constraint from $\mathcal{B}(B_c^+ \to \tau^+\nu_\tau)$ was also imposed. Here, we show the results using the numerical values of C_{V_L}, C_{S_L} and C_{S_R} from Fits 1 and 2 tabulated in Table 3 of [54] (including $F_L^{D^*}$) with $\mathcal{B}(B_c^+ \to \tau^+\nu_\tau) \leq 30\%$. In this paper, we do not consider Fit 3 as it is found to be already disregarded by the measured differential distributions. For all the three decay modes, NP scenarios using Fits 1 and 2 are clearly distinguishable. It is observed that predictions with Fit 1 are much closer to the SM than those with Fit 2, which is similar to the observations of Murgui et al. for b-meson modes.

5 Summary and conclusion

We have analyzed the semileptonic b-baryon decays $\Xi_b \to \Xi_c\tau^-\bar{\nu}_\tau$ and $\Sigma_b \to \Sigma_c^{(*)}\tau^-\bar{\nu}_\tau$ within a model-independent effective theory framework, consisting of both SM and NP contributions. The helicity amplitudes method was used to describe the hadronic transitions. Form factors expressed in terms of Isgur–Wise functions in the heavy quark limit have been adopted to parametrize the decay amplitudes. These form factors were obtained within the relativistic quark model. The SM predictions in the relativistic quark model and those obtained using lattice QCD results were first compared for an assessment of the validity of the different approaches. It was found that form factors calculated in RQM and on the lattice are compatible at the zero recoil point of the final baryon. The total decay rate, branching ratios and R_{Λ_c} differed slightly in the two cases. On analyzing NP effects, we considered one new coupling at a time and using a χ^2 fitting, best-fit values of these couplings were obtained. Predictions for the q^2-dependence of various observables such as the differential branching ratio, ratio of branching fractions, forward-backward asymmetry of the charged lepton, convexity parameter and lepton polarization have been presented in both the SM and NP scenarios. In order to determine the allowed NP parameter space, we imposed a 1σ constraint from the experimental measurements of the LFU ratios $R_{D^{(*)}}$, $R_{J/\psi}$, the D^{*-} polarization $F_L^{D^*}$ and the τ polarization $P_\tau^{D^*}$. We observed NP sensitivity for most of the observables of interest, with the deviations from the SM prediction being more discernible in the scenario with new scalar couplings than that with new vector couplings. In particular, observables such as the ratio of branching fractions, convexity parameter and lepton polarization were found to be more sensitive to the new contributions for some of the decay modes considered. Using previously obtained significant fits of the new couplings, predictions for the different q^2-dependent observables were also presented. It was observed that NP with these fits mostly displayed distinct variations from the SM. Hence, the study of semileptonic $b \to c\ell^-\bar{\nu}_\ell$ transitions of half-integer spin b-baryons such as those considered in this work can be invaluable in revealing the presence and ascertaining the exact nature of NP. Also, the study of such baryon modes augments that of the b-meson modes as they furnish a complementary environment in the search for NP.

Acknowledgements C. P. Haritha would like to acknowledge UGC, Govt. of India for the NFOBC fellowship.

Data Availability Statement This manuscript has no associated data or the data will not be deposited. [Authors' comment: Data used in the manuscript has been cited and can be found in the references section. All results are given within the main text itself. There is no other associated data.]

Funded by SCOAP[3]. SCOAP[3] supports the goals of the International Year of Basic Sciences for Sustainable Development.

A Form factors for the semileptonic $\Lambda_b \to \Lambda_c$ decay

The form factors used in Eq. (3) are related to those used in [41] by the following relations.

$$
\begin{aligned}
f_\perp(q^2) &= F_1(q^2)\\
f_+(q^2) &= F_1(q^2)+\left[\frac{(m_{B_b}+m_{B_c})^2-q^2}{2m_{B_b}(m_{B_b}+m_{B_c})}\right]F_2(q^2)\\
&\quad+\left[\frac{(m_{B_b}+m_{B_c})^2-q^2}{2m_{B_c}(m_{B_b}+m_{B_c})}\right]F_3(q^2)\\
f_0(q^2) &= F_1(q^2)+\left[\frac{(m_{B_b}^2-m_{B_c}^2)+q^2}{2m_{B_b}(m_{B_b}-m_{B_c})}\right]F_2(q^2)\\
&\quad+\left[\frac{(m_{B_b}^2-m_{B_c}^2)-q^2}{2m_{B_c}(m_{B_b}-m_{B_c})}\right]F_3(q^2)\\
g_\perp(q^2) &= G_1(q^2)
\end{aligned}
$$

$$
\begin{aligned}
g_+(q^2) &= G_1(q^2) - \left[\frac{(m_{B_b} - m_{B_c})^2 - q^2}{2m_{B_b}(m_{B_b} - m_{B_c})}\right] G_2(q^2) \\
&\quad - \left[\frac{(m_{B_b} - m_{B_c})^2 - q^2}{2m_{B_c}(m_{B_b} - m_{B_c})}\right] G_3(q^2) \\
g_0(q^2) &= G_1(q^2) - \left[\frac{(m_{B_b}^2 - m_{B_c}^2) + q^2}{2m_{B_b}(m_{B_b} + m_{B_c})}\right] G_2(q^2) \\
&\quad - \left[\frac{(m_{B_b}^2 - m_{B_c}^2) - q^2}{2m_{B_c}(m_{B_b} + m_{B_c})}\right] G_3(q^2) \qquad \text{(A.1)}
\end{aligned}
$$

References

1. Y. Amhis et al. [HFLAV Collaboration], (2022). arXiv:2206.07501 [hep-ex]
2. D. Bigi, P. Gambino, Phys. Rev. D **94**, 094008 (2016)
3. F.U. Bernlochner, Z. Ligeti, M. Papucci, D.J. Robinson, Phys. Rev. D **95**, 115008 (2017) [Erratum: Phys. Rev. D **97**, 059902 (2018)]
4. S. Jaiswal, S. Nandi, S.K. Patra, JHEP **12**, 060 (2017)
5. M. Bordone, M. Jung, D. van Dyk, Eur. Phys. J. C **80**, 74 (2020)
6. P. Gambino, M. Jung, S. Schacht, Phys. Lett. B **795**, 386 (2019)
7. J.P. Lees et al. [BaBar Collaboration], Phys. Rev. Lett. **123**, 091801 (2019)
8. R. Aaij et al. [LHCb Collaboration], Phys. Rev. Lett. **120**, 121801 (2018)
9. R. Dutta, A. Bhol, Phys. Rev. D **96**, 076001 (2017)
10. S. Hirose et al. [Belle Collaboration], Phys. Rev. Lett. **118**, 211801 (2017)
11. S. Hirose et al. [Belle Collaboration], Phys. Rev. D **97**, 012004 (2018)
12. A. Abdesselam et al. [Belle Collaboration], in 10th International Workshop on the CKM Unitarity Triangle (2019). arXiv:1903.03102 [hep-ex]
13. A. Crivellin, C. Greub, A. Kokulu, Phys. Rev. D **86**, 054014 (2012)
14. A. Celis, M. Jung, X.-Q. Li, A. Pich, JHEP **01**, 054 (2013)
15. A. Crivellin, J. Heeck, P. Stoffer, Phys. Rev. Lett. **116**, 081801 (2016)
16. A. Greljo, G. Isidori, D. Marzocca, JHEP **07**, 142 (2015)
17. S.M. Boucenna, A. Celis, J. Fuentes-Martin, A. Vicente, J. Virto, Phys. Lett. B **760**, 214 (2016)
18. I. Doršner, S. Fajfer, N. Košnik, I. Nišandžić, JHEP **11**, 084 (2013)
19. Y. Sakaki, M. Tanaka, A. Tayduganov, R. Watanabe, Phys. Rev. D **88**, 094012 (2013)
20. M. Bauer, M. Neubert, Phys. Rev. Lett. **116**, 141802 (2016)
21. R. Barbieri, G. Isidori, A. Pattori, F. Senia, Eur. Phys. J. C **76**, 67 (2016)
22. T. Aaltonen et al. [CDF Collaboration], Phys. Rev. Lett. **99**, 052002 (2007)
23. V.M. Abazov et al. [D0 Collaboration], Phys. Rev. Lett. **99**, 052001 (2007)
24. R. Aaij et al. [LHCb Collaboration], Phys. Rev. Lett. **113**, 032001 (2014)
25. R. Aaij et al. [LHCb Collaboration], Phys. Lett. B **736**, 154 (2014)
26. R. Aaij et al. [LHCb Collaboration], Phys. Rev. D **89**, 032001 (2014)
27. R. Aaij et al. [LHCb Collaboration], Phys. Rev. Lett. **113**, 242002 (2014)
28. R. Aaij et al. [LHCb Collaboration], Phys. Rev. Lett. **115**, 241801 (2015)
29. R. Aaij et al. [LHCb Collaboration], Phys. Rev. Lett. **118**, 071801 (2017)
30. R. Aaij et al. [LHCb Collaboration], Phys. Lett. B **772**, 265 (2017)
31. R. Aaij et al. [LHCb Collaboration], JHEP **02**, 098 (2018)
32. R. Aaij et al. [LHCb Collaboration], Phys. Rev. D **99**, 052006 (2019)
33. T.A. Aaltonen et al. [CDF Collaboration], Phys. Rev. D **89**, 072014 (2014)
34. T. Aaltonen et al. [CDF Collaboration], Phys. Rev. Lett. **99**, 202001 (2007)
35. T. Aaltonen et al., (CDF Collaboration). Phys. Rev. D **85**, 092011 (2012)
36. R. Aaij et al. [LHCb Collaboration], Phys. Rev. Lett. **122**, 012001 (2019)
37. H.-W. Ke, N. Hao, X.-Q. Li, Eur. Phys. J. C **79**, 540 (2019)
38. J.G. Korner, M. Kramer, D. Pirjol, Prog. Part. Nucl. Phys. **33**, 787 (1994)
39. M.A. Ivanov, V.E. Lyubovitskij, J.G. Korner, P. Kroll, Phys. Rev. D **56**, 348 (1997)
40. M.A. Ivanov, J.G. Korner, V.E. Lyubovitskij, A.G. Rusetsky, Phys. Rev. D **59**, 074016 (1999)
41. W. Detmold, C. Lehner, S. Meinel, Phys. Rev. D **92**, 034503 (2015)
42. R.L. Singleton, Phys. Rev. D **43**, 2939 (1991)
43. H.-Y. Cheng, B. Tseng, Phys. Rev. D **53**, 1457 (1996) [Erratum: Phys. Rev. D 55, 1697 (1997)]
44. F. Cardarelli, S. Simula, Phys. Rev. D **60**, 074018 (1999)
45. C. Albertus, E. Hernandez, J. Nieves, Phys. Rev. D **71**, 014012 (2005)
46. H.-W. Ke, X.-H. Yuan, X.-Q. Li, Z.-T. Wei, Y.-X. Zhang, Phys. Rev. D **86**, 114005 (2012)
47. D. Ebert, R.N. Faustov, V.O. Galkin, Phys. Rev. D **73**, 094002 (2006)
48. R.N. Faustov, V.O. Galkin, Phys. Rev. D **98**, 093006 (2018)
49. S. Shivashankara, W. Wu, A. Datta, Phys. Rev. D **91**, 115003 (2015)
50. R. Dutta, Phys. Rev. D **93**, 054003 (2016)
51. X.Q. Li, Y.D. Yang, X. Zhang, JHEP **02**, 068 (2017)
52. A. Datta, S. Kamali, S. Meinel, A. Rashed, JHEP **08**, 131 (2017)
53. E. Di Salvo, F. Fontanelli, Z.J. Ajaltouni, Int. J. Mod. Phys. A **33**, 1850169 (2018)
54. C. Murgui, A. Pe nuelas, M. Jung, A. Pich, JHEP **09**, 103 (2019)
55. M. Blanke, A. Crivellin, S. de Boer, T. Kitahara, M. Moscati, U. Nierste, I. Nišandžić, Phys. Rev. D **99**, 075006 (2019)
56. X.-L. Mu, Y. Li, Z.-T. Zou, B. Zhu, Phys. Rev. D **100**, 113004 (2019)
57. A. Ray, S. Sahoo, R. Mohanta, Phys. Rev. D **99**, 015015 (2019)
58. F.U. Bernlochner, Z. Ligeti, D.J. Robinson, W.L. Sutcliffe, Phys. Rev. D **99**, 055008 (2019)
59. P. Böer, A. Kokulu, J.-N. Toelstede, D. van Dyk, JHEP **12**, 082 (2019)
60. N. Penalva, E. Hernández, J. Nieves, Phys. Rev. D **100**, 113007 (2019)
61. N. Penalva, E. Hernández, J. Nieves, Phys. Rev. D **101**, 113004 (2020)
62. Q.-Y. Hu, X.-Q. Li, Y.-D. Yang, D.-H. Zheng, JHEP **02**, 183 (2021)
63. N. Penalva, E. Hernández, J. Nieves, JHEP **06**, 118 (2021)
64. R. Dutta, Phys. Rev. D **97**, 073004 (2018)
65. N. Rajeev, R. Dutta, S. Kumbhakar, Phys. Rev. D **100**, 035015 (2019)
66. J. Zhang, X. An, R. Sun, J. Su, Eur. Phys. J. C **79**, 863 (2019)
67. J.-H. Sheng, J. Zhu, X.-N. Li, Q.-Y. Hu, R.-M. Wang, Phys. Rev. D **102**, 055023 (2020)
68. H.D. Politzer, M.B. Wise, Phys. Lett. B **206**, 681 (1988)
69. N. Isgur, M.B. Wise, Phys. Lett. B **232**, 113 (1989)
70. G.P. Lepage, B. Thacker, Nucl. Phys. B Proc. Suppl. **4**, 199 (1988)
71. E. Eichten, B.R. Hill, Phys. Lett. B **234**, 511 (1990)
72. B. Grinstein, Nucl. Phys. B **339**, 253 (1990)
73. H. Georgi, Phys. Lett. B **240**, 447 (1990)
74. F. Hussain, J.G. Korner, K. Schilcher, G. Thompson, Y.L. Wu, Phys. Lett. B **249**, 295 (1990)

75. M. Neubert, Phys. Rep. **245**, 259 (1994)
76. A. Kadeer, J.G. Korner, U. Moosbrugger, Eur. Phys. J. C **59**, 27 (2009)
77. T. Gutsche, M.A. Ivanov, J.G. Korner, V.E. Lyubovitskij, P. Santorelli, Phys. Rev. D **87**, 074031 (2013)
78. T. Gutsche, M.A. Ivanov, J.G. Körner, V.E. Lyubovitskij, P. Santorelli, Phys. Rev. D **88**, 114018 (2013)
79. W. Buchmuller, D. Wyler, Nucl. Phys. B **268**, 621 (1986)
80. B. Grzadkowski, M. Iskrzynski, M. Misiak, J. Rosiek, JHEP **10**, 085 (2010)
81. J. Aebischer, A. Crivellin, M. Fael, C. Greub, JHEP **05**, 037 (2016)
82. V. Cirigliano, J. Jenkins, M. Gonzalez-Alonso, Nucl. Phys. B **830**, 95 (2010)
83. R. Alonso, B. Grinstein, J. Martin Camalich, JHEP **10**, 184 (2015)
84. R.-X. Shi, L.-S. Geng, B. Grinstein, S. Jäger, J. Martin Camalich, JHEP **12**, 065 (2019)
85. T. Gutsche, M.A. Ivanov, J.G. Körner, V.E. Lyubovitskij, P. Santorelli, Phys. Rev. D **90**, 114033 (2014) [Erratum: Phys. Rev. D **94**, 059902 (2016)]
86. T. Gutsche, M.A. Ivanov, J.G. Körner, V.E. Lyubovitskij, P. Santorelli, N. Habyl, Phys. Rev. D **91**, 074001 (2015) [Erratum: Phys. Rev. D **91**, 119907 (2015)]
87. R.N. Faustov, V.O. Galkin, X.W. Kang, Phys. Rev. D **106**, 013004 (2022)
88. R.N. Faustov, V.O. Galkin, Phys. Rev. D **94**, 073008 (2016)
89. P. Zyla et al. [Particle Data Group], PTEP **2020**, 083C01 (2020)
90. R. Alonso, B. Grinstein, J. Martin Camalich, Phys. Rev. Lett. **118**, 081802 (2017)
91. I. Caprini, L. Lellouch, M. Neubert, Nucl. Phys. B **530**, 153–181 (1998)
92. M. Okamoto, C. Aubin, C. Bernard, C.E. DeTar, M. Di Pierro, A.X. El-Khadra, S. Gottlieb, E.B. Gregory, U.M. Heller, J. Hetrick et al., Nucl. Phys. B Proc. Suppl. **140**, 461–463 (2005)
93. R. Watanabe, Phys. Lett. B **776**, 5 (2018)
94. W.F. Wang, Y.Y. Fan, Z.J. Xiao, Chin. Phys. C **37**, 093102 (2013)
95. T.W. Chiu et al. [TWQCD], Phys. Lett. B **651**, 171–176 (2007)